Improved *p*- and *n*-type thin-film microstructures for thermoelectricity

J.P. Carmo, L.M. Goncalves and J.H. Correia

Improved microstructures based on thin-films of *n*-type bismuth telluride (Bi_2Te_3) and *p*-type antimony telluride (Sb_2Te_3) to convert temperature differences in electricity are presented. The microstructures are obtained by thin-film deposition, applying the co-evaporation method to the bismuth/antimony and telluride materials. Measurements demonstrated the superior thermoelectric features of the obtained films when compared with the most recent thermoelectric thin-film deposition. Measurements show that the deposited films present thermoelectric properties comparable to those reported for the same materials in bulk form, as is the case of the materials used in conventional macro-scale Peltier modules. The absolute values of the Seebeck coefficient are in the range $150-250\ \mu VK^{-1}$ and the in-plane electrical resistivity is in the $7-15\ \mu \Omega m$ range. Measurements for the Bi_2Te_3 and Sb_2Te_3 films also show figures of merit at room temperatures of 0.84 and 0.5, and power factors of 4.87 and 2.81 $mWK^{-2}m^{-1}$, respectively. These microstructures are used for the fabrication of thermoelectric microgenerators to supply stand-alone microsystems with power consumption that ranges from cents of μW to a few mW.

Introduction: Providing a sustainable supply of energy to the world's population will become a major societal problem for the 21st century as fossil fuel supplies decrease and world demand increases [1]. Thermoelectric phenomena, which involve the conversion between thermal and electrical energy, and provide a method for heating and cooling materials, are expected to play an increasingly important role in meeting the energy challenge of the future [1]. Therefore, thermoelectric materials are attractive for a wide range of applications because they can make thermal-to-electric or electric-to-thermal energy conversion in a direct way without moving mechanical parts [2]. Also, it provides compact and distributed power, quiet operation, and is usually environmentally friendly. To make these processes as efficient as possible, the need for suitable materials is a mandatory requirement. The highest performance is obtained in the presence of heavily-doped semiconductors, such as bismuth telluride or silicon germanium. For the case of semiconductors, the most desirable situation is when the base materials are both *n*- and *p*-doped in order to apply the same material system on both sides of the junctions [3]. This Letter compares the improved *n*-type bismuth telluride (Bi_2Te_3) and *p*-type antimony telluride (Sb_2Te_3) microstructures with state-of-the-art deposited thermoelectric materials [4–7].

Deposition of thin-films: Thermoelectric films were fabricated by the thermal co-evaporation technique in a high-vacuum chamber (with a base pressure of $\sim 1 \times 10^{-6}$ Torr). Two large molybdenum boats (baffled boxes, with a volume of 4 cm^3) are used at the same time, one for each of the elementary materials required to produce the desired compound. The power applied to each boat is controlled independently, using two computed proportional-integral derivative (PID) controllers to maintain the deposition rate at user-defined constant values, during the deposition process. Two thickness monitors (quartz crystal oscillators) are carefully placed inside the chamber in such a way that each of them receives material only from the boat it is monitoring. The mixing of both materials is avoided with a metal sheet placed between the two boats. Substrates were heated to the temperature set point (T_{sub}) in the range 150–270°C.

The influence of the evaporation rate of each material on the thermoelectric properties of the compounds was analysed, taking into account the individual evaporation ratio of each co-evaporation session. The evaporation ratio, $R = Fr_{Te}/Fr_{Bi,Sb}$, is defined as the amount (in volume of the deposited film) of tellurium (Te) divided by the amount of bismuth (Bi), or antimony (Sb), that arrives at the substrate during deposition. The highest power factor, PF, was obtained with a Bi (or Sb) evaporation rate of 2 Ås^{-1} and a Te evaporation rate of 6–7 Ås^{-1}, which corresponds to an evaporation ratio in the range 3–3.5.

The best films were obtained at $T_{sub} = 270$°C. For $T_{sub} > 290$°C films with high mechanical stress and/or poor adhesion were obtained owing to the degradation of the polyimide substrate. Finally, it must be noted that all films were deposited on a polyimide (kapton) foil with a thickness of 25 μm. The SEM cross-sectional and surface images of the films confirm their polycrystalline structure. The effect of substrate temperature on polycrystalline morphology can be seen in Fig. 1.
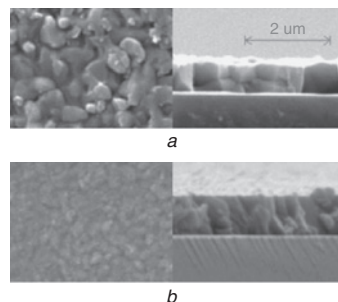

Fig. 1 *SEM top view (left) and cross-section (right) images*
a Bi_2Te_3 thin film
b Sb_2Te_3 thin-film

Results: The in-plane electrical resistivity, carrier concentration and Hall mobility were measured at room temperature using the conventional four probe van der Pauw geometry. A DC magnetic field of 80 mT was applied for Hall measurements. The Seebeck coefficient, α, was measured by connecting one side of the film to a heated metal block at a fixed temperature, and the other side to a heatsink kept at room temperature, with a temperature difference between both sides below 10°C. A spot of $\simeq 5 \times 5$ mm is considered for electrical properties. The thermal conductivity ($Wm^{-1}K^{-1}$) was measured and was obtained as 1.3 and 1.8 $Wm^{-1}K^{-1}$ for the Bi_2Te_3 and Sb_2Te_3 films (which were deposited as conditions to obtain the maximum power factor), respectively. The measurements of the Seebeck coefficient were made, by connecting one side of the film to a fixed temperature (heated metal block) and the other side to a heatsink at room temperature. These measurements showed an absolute value of the Seebeck coefficient in the range $150-250\ \mu VK^{-1}$, and an in-plane electrical resistivity of $7-15\ \mu \Omega m$. The measurements also showed for Bi_2Te_3 and Sb_2Te_3 films, figures of merit (ZT) at room temperature of 0.84 and 0.5, and power factors of 4.87 and 2.81 $mWK^{-2}m^{-1}$, respectively. Tables 1 and 2 show the results of these measurements in selected samples of Bi_2Te_3 and Sb_2Te_3 films, as well as the corresponding ZT. The Tables list the PF for the selected samples of Bi_2Te_3 and Sb_2Te_3.

Table 1: Properties of selected *n*-type Bi_2Te_3 films

Film	α (μVK^{-1})	ρ ($\mu \Omega m$)	PF ($mWK^{-2}m^{-1}$)	ZT at 300K
1	−74	5.70	0.96	0.19
2	−180	16.6	1.95	0.40
3	−156	11.3	2.16	0.43
4	−152	13.4	1.72	0.34
5	−248	12.6	4.87	0.97
6	−220	10.6	4.57	0.91

Table 2: Properties of selected *p*-type Sb_2Te_3 films

Film	α (μVK^{-1})	ρ ($\mu \Omega m$)	PF ($mWK^{-2}m^{-1}$)	ZT at 300K
1	91	7.60	1.09	0.22
2	140	14.0	1.40	0.28
3	156	9.20	2.66	0.53
4	188	12.6	2.81	0.56

Table 3: For *n*-type thermoelectric materials, comparison of experimental results obtained with *n*-type Bi_2Te_3 sample and with state-of-the-art [4–7]

Deposition method	α (μVK^{-1})	σ (Scm^{-1})	PF $\times 10^{-3}$ ($WK^{-2}m^{-1}$)	Carrier concentration (cm^{-1})	Reference
Co-evaporation	−248	793.7	4.87	$3-20 \times 10^{19}$	This work
Flash evaporation	−252	549.5	3.49		[4]
DC magnetron sputtering	−201	29.4	0.12		[5]
RF magnetron sputtering	−248	1.39	0.41	1.25×10^{21}	[6]

Discussion: Table 3 (for *n*-type materials) and Table 4 (for *p*-type materials) compare the experimental results of the proposed microstructures with those obtained from the most recent work cited in the literature [4–7]. In both Tables, the shaded cells reveal the absence of values for the carrier concentration in the reference literature [4, 7].

Table 4: For *p*-type thermoelectric materials, comparison of experimental results obtained with *p*-type Sb_2Te_3 sample and with state-of-the-art [4–7].

Deposition method	α (μVK^{-1})	σ (Scm^{-1})	$PF \times 10^{-3}$ ($WK^{-2} m^{-1}$)	Carrier concentration (cm^{-1})	Reference
Co-evaporation	188	793.7	2.81	$1-7 \times 10^{19}$	This work
DC magnetron Sputtering	304	2.22	21×10^{-2}		[5]
Electrodeposition	320	200	2.04	6×10^{21}	[7]

From Table 3 for the case of *n*-type materials, it is notorious for superior performance in all thermoelectric aspects (α, σ and PF) of the proposed thermoelectric microstructures when compared to those deposited with the flash evaporation, the DC and RF magnetron sputtering techniques. After the co-deposition of both *n*- and *p*-type thermoelectric materials, the annealing process was not performed to prevent the re-evaporation of tellurium occurring. This precaution avoids possible decreases in the thermoelectric performances of deposited films. Also, the annealing improves the crystalline structure of films, which means that the carrier concentration of the same films is also improved. This is a possible explanation for the lowest carrier concentration of the deposited films.

For the case of *p*-type materials, in spite of DC magnetron sputtering and electrodeposition, techniques achieve high Seebeck coefficients (α) when compared with the selected sample, the conductivity and principally, the power factor is the highest when compared with the other works [5, 7].

Conclusion: Thermoelectric microstructures are presented based on ZT Bi_2Te_3 and Sb_2Te_3 materials that were deposited by co-evaporation, in the form of thin-films. Experiments and further comparison with more recent state-of-the-art microstructures have demonstrated the superior thermoelectric performance of the proposed microstructures. This is another reason why these microstructures are suitable in the construction of thermoelectric scavenging systems to power stand-alone microsystems with power consumption ranges from cents of μW to a few mW.

J.P. Carmo, L.M. Goncalves and J.H. Correia (*University of Minho, Department of Industrial Electronics, Campus Azurem, 4800-058 Guimaraes, Portugal*)

E-mail: jcarmo@dei.uminho.pt

References

1 Dresslhaus, M.S., Chen, G., Tang, M.Y., Yang, R., Lee, H., Wang, D., Ren, Z., Fleurial, J.-P., and Gogna, P.: 'New directions for low-dimensional thermoelectric materials', *Adv. Mater.*, 2007, **19**, pp. 1–12

2 Bell, L.: 'Cooling, heating, generating power, and recovering waste heat with thermoelectric systems', *Science*, 2008, **321**, pp. 1457–1461

3 Wijngaards, D.L., Kong, S.M., Bartek, M., and Wolffenbuttel, R.F.: 'Design and fabrication of on-chip integrated polySiGe and polySi Peltier devices', *Sens. Actuators A: Phys.*, 2000, **85**, pp. 316–323

4 Takashiri, M., Miyazaki, K., and Tsukamoto, H.: 'Structural and thermoelectric properties of fine-grained $Bi_{0.4}Te_{3.0}Sb_{1.6}$ thin-films preferred orientation deposited by flash evaporation method', *Thin Solid Films*, 2008, **516**, pp. 6336–6343

5 Bourgault, D., Garampon, C., Caillault, N., Carbone, L., and Aymami, J.A.: 'Thermoelectric properties of n-type $Bi_2Te_{2.7}Se_{0.3}$ and p-type $Bi_{0.5}Sb_{1.5}Te_3$ thin-films deposited by direct current magnetron sputtering', *Thin Solid Films*, 2008, **516**, pp. 8579–8583

6 Huang, H., Luan, W., and Tu, S.: 'Influence of annealing on thermoelectric properties of bismuth telluride films grown via radio frequency magnetron sputtering', *Thin Solid Films*, 2009, **517**, pp. 3731–3734

7 Lim, S., Kim, M., and Oh, T.: 'Thermoelectric properties of the bismuth-antimony-telluride and the antimony-telluride films processed by electrodeposition for micro-device applications', *Thin Solid Films*, 2009, **517**, pp. 4199–4203